International Journal of Applied Engineering Research ISSN 0973-4562 Volume 10, Number 19 (2015) pp 40234-40240

Classification of breast masses in mammogram images through Shearlet transform and SVM

Manoharan.

Research scholar, M. S University, Tirunelveli, magann1968@yahoo. co. in

R SubiStalin. M,

Research scholar, M. S University Tamil Nadu, India, stalin2k7@gmail. Com

Kalaimagal. R

Research supervisor, Govt. Arts College for Men, Nandanam Tirunelveli, Tamil Nadu, India Chennai, Tamil Nadu, India kalai_magal@rediffmail. com

Abstract

This paper presents a methodology for the detection of breast masses in mammogram images through shearlet transform and support vector machine (SVM). The proposed system focuses on two methods of how to segment the underlying masses in the noisy mammograms using shearlet transformation function and another is to classify the features that depict the masses in breast mammogram using SVM. The automatic mass detection includesthree stages (1) Image enhancement and contrast adjustment, (2) Segmentation (ROI) and (3) Classification (SVM classifier). The proposed approach is applied to MIAS mini image dataset and their findings depict the normal and severity of abnormal based on benign and malignant. The initial preprocessing stage includes the image enhancement using shearlet transform for de-noisingthroughshearlet filters to remove the white noise and contrast adjustment. These regions have their shapes analyzed through the shape descriptors. Support vector machines were used to classify the candidate regions as masses or non-masses.

Keywords: Image segmentation, Support vector machine, Shearlet transform, mammography

Introduction

Breast cancer is the cancer that develops from breast tissue. Breast cancer is a very commonly diagnosed cancerous abnormality in that one third of all cancers detected among women is related to breast. Current technologies are very effective to treat early-stage breast cancers, which makes the early detection a crucial task. Breast cancer is one of the most dangerous types of cancer among women all over the world. It happens to over 11% women during their life time. There are a number of contributing factors such as: (1) a familial history of breast cancer, especially with breast cancer in her mother or sister; (2) the woman's first child birth is after 30 years of age; (3) the woman ingests foods with high fat or calorie content; (4) the woman's chest has been subjected to radioactivity several times; and (5) the woman has had ovarian or endometrial cancer. Early detection can play an effective role in prevention, particularly by the most reliable detection technology known as mammography. IMAGE segmentation is a process of dividing an image into different regions such that each region is nearly homogeneous. Shearlet is a genuinely multidimensional and non-isotropic version of the traditional wavelet transform method, with an advantage in superior directional sensitivity at various scales. Shearlet has been widely used in image processing, such as sparse image representation, edge detection, imagedenoising and image fusion. **[1]**AshkanTashk et al. (2015) proposed an automatic detection of breast cancer mitotic cells based on the combination of textural, statistical features like completed local binary pattern (CLBP) as textural features, statistical moment entropy (SME) and stiffness matrix (SM) as a mathematical model which includes geometric, morphometric and shape-based feature. **[2]**Chien-Shun Lo and Chuin-Mu Wang (2012) used a support vector machine (SVM) to breast multi-spectral magnetic resonance images to classify the tissues of the breast and stated that the SVM method is a promising and effective spectral technique for MR image classification. **[3]**Defeng Wang et al. (2009) proposed an automatic detection of breast cancers in mammograms using structured support vector machines (s-SVM). They extracted various features like, curvilinear features, Gabor features and multi resolution features from the sample images. **[4]**BetsabehTanoori et al. (2011) presented the segmentation of brain MRI images using vector field convolution (VFC) and support vector machine (SVM). They followed two step segmentation process, first remove skull and non-brain regions and the nest step segmentation of the brain into GM, WM and CSF regions, based on the SVM classifier with a simple feature selection and a high accuracy. **[5]**Hong-Ying Yang et al. (2012) presented an effective color image segmentation approach based on pixel classification with least squares support vector machine (LS-SVM) and stated that proposed segmentation method was good agreement in comparison with the state-of-the-art segmentation. **[6]**Mohsen Keshani et al. (2013) presented a novel method for lung nodule detection, segmentation and recognition using computed tomography (CT) images. Nodules were detected by the support vector machine (SVM) classifier using efficient 2D stochastic and 3D anatomical features. They classified the lung tissues into four classes namely lung wall, parenchyma,

bronchioles and nodules. From the experimental results, solid and non-solid and cavitary nodules were detected with an overall detection rate of 89%. **[7]**Teresa Wu et al. (2012) proposed an automated method, called prior feature Support Vector Machine-Markov Random Field (pSVMRF), to segment three-dimensional mouse brain Magnetic Resonance Microscopy (MRM) images. They validated the proposed method using MR imaging of unstained and actively stained mouse brain specimens, and compare segmentation accuracy with two existing methods: eMRF and MRF. Experimental results suggest that Segmentation accuracy for new strains is 80% for hippocampus, and caudate putamen, indicating that pSVMRF is a promising approach for phenotyping mouse models of human brain disorders. **[8]**Xiang-Yang Wang et al. (2011) presented color image segmentation using automatic pixel classification with support vector machine (SVM). They trained the SVM model using fuzzy c-means clustering (FCM) with the extracted pixel-level features. From the experimental results, they stated that the proposed method has a very effective segmentation results and computational behavior, and decreases the time and increases the quality of color image segmentation in compare with the state-of-the-art segmentation. **[9]**Ye Chen et al. (2014) developed a novel local feature based support vector machine (SVM) approach to detect brain structural changes as potential biomarkers. They used FBM based approach in the image feature preprocess step to remove noise features and identify disease-related and healthy-related features. Also they demonstrated the wide applicability of this approach to neurological and psychiatric diseases by applying it to three different diseases: Alzheimer's disease, Parkinson's disease and bipolar disorder. From the experimental results, they found that the classification accuracy ranges between 70% and 87%. **[10]**Wener Borges Sampaio et al. (2011) presented a computational methodology to detect breast masses in mammogram images. They used cellular neural networks to segment the regions contain masses and these regions shapes were analyzed through shape descriptors and their textures analyzed through geostatistic functions. They used Support vector machines to classify the candidate regions as masses or non-masses, with sensitivity of 80%. **[11]**Mohamed MeselhyEltoukhy et al. (2010) presented the comparative study between wavelet and curvelet transform for breast cancer diagnosis in digital mammogram. They decomposed the mammogram images into different resolution levels through multi resolution analysis. The performance of the classifier evaluated using a 2×5-fold cross validation followed by a statistical analysis. The results reported that curvelet transform produces better results compare with wavelet transform. **[12]**FatemehMoayedi et al. (2010) proposed contourlet-based texture analysis along with the geometrical and statistical features and employed SEL weighted SVM, SVFNN and kernel SVM classifiers to detect and classify the breast masses into benign and malignant cases and reported that Contourlet based feature extraction in conjunction with the state-of-art classifiers construct a powerful efficient and practical approach for automatic mass classification of mammograms. **[13]**Shichong Zhou et al. (2013)proposed a novel method that extracts texture feature descriptors based on shearlet transform to improve the performance of discriminating benign breast mass from malignant tumor in ultrasound image. The experimental results indicated that the shearlet based texture feature could effectively characterize breast tumors in ultrasound image than other features extracted from wavelet, contourlet and curvelet and GLCM methods. They reported that the shearlet based texture feature has a better potential to be used in breast ultrasound CAD. Our objective is to develop an automated imaging system for mass classification of digital mammograms. Mass classification requires a preprocessing step of segmenting the input image into disjoint areas, such as the breast region, background, and redundant labels and content text. Also namely the support vector machines (SVM) were adopted to evaluate the consistency of the discriminative power of the shearlet-based texture feature descriptors.

Materials and methods

Data acquisition

In the present study, a set of images provided by the Mammographic Image Analysis Society (MIAS) is used in applying the proposed technique. These images were previously investigated and labeled by an expert radiologist based on technical experience and biopsy. The dataset is selected due to the various cases it includes. The dataset is composed of 322 mammograms of right and left breast, from 161 patients, where 51 were diagnosed as malignant, 64 as benign and 207 as normal. The abnormalities are classified into micro calcification, circumscribed mass, spiculated mass, ill-defined mass, architectural distortion, and asymmetry. The original mammograms are 1024*1024 pixels, and almost 50% of the whole image comprised of the background with a lot of noise.

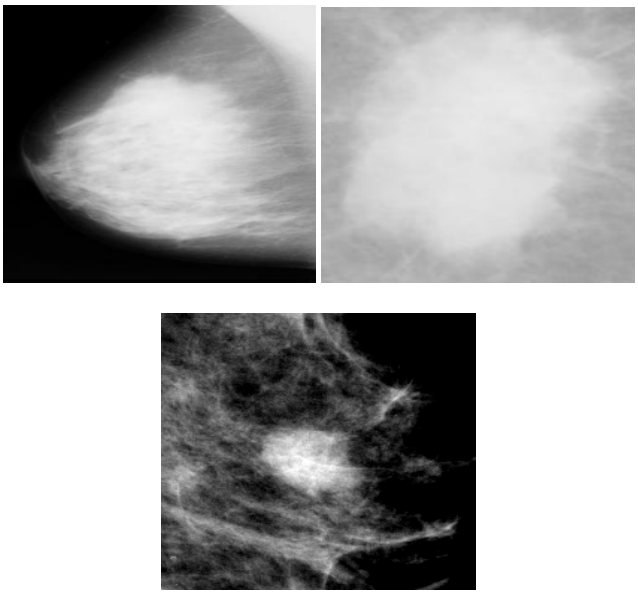

Figure 1. (a) Initial image, (b) Cropped image, (c) Contrast adjusted image

Preprocessing

Each mammographic sample image is preprocessed prior to feature extraction. We first use the median filtering to reduce the overall noise caused by statistics of X-ray quantum absorption. Then the filtered sample images are enhanced using a physics-based mammogram enhancement method introduced in, which models the X-ray physics of the imaging process.

Image enhancement

Image cropping includes the removal of letters present in the image to identify the class category. Then the image is resized to the equal pixels of rows and columns.

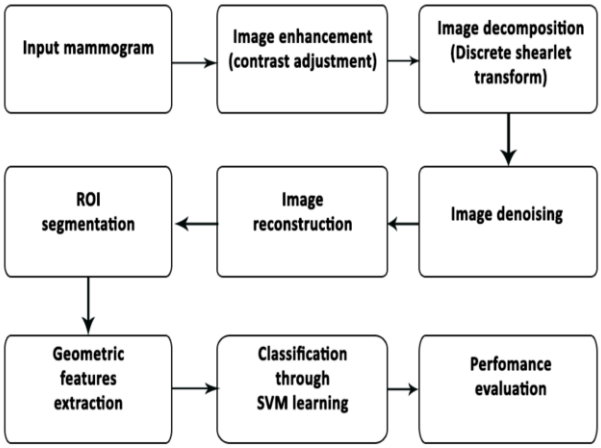

Figure 2. Process Flow diagram of the proposed method

Contrast adjustment

Since shearlet provide nearly optimally sparse representations for a large class of functions that are useful to model natural images, many image processing methods benefit from their use. In particular, the error rates of data estimation from noise are highly dependent on the sparsity properties of the representation, so that many successful applications of shearlet center around restoration tasks such as denoising and inverse problems. Other imaging problems, where also the application of the shearlet representation turns out to be very beneficial, include image enhancement, image separation, edge detection, and estimation of the geometric features of an object.

Discrete shearlet transformation

It will be convenient to describe the collection of shearlets presented in a way which is more suitable to derive its numerical implementation. For $\xi = (\xi 1, \xi 2) \in \hat{\mathbb{R}}^2$, $j \geq 0$, and $l = -2^j,\ldots, 2^j - 1$, let

$$W^{(0)}{}_{j,l}(\xi) = \begin{cases} \hat{\psi}_2\left(2^j \frac{\xi_2}{\xi_1} - 1\right)\chi D_0(\xi) + \hat{\psi}_2\left(2^j \frac{\xi_1}{\xi_2} - l + 1\right)\chi D_1(\xi) & \text{if } l = -2^j \\ \hat{\psi}_2\left(2^j \frac{\xi_2}{\xi_1} - l + 1\right)\chi D_0(\xi) + \hat{\psi}_2\left(2^j \frac{\xi_1}{\xi_2} - l\right)\chi D_1(\xi) & \text{if } l = 2^j - 1 \\ \hat{\psi}_2\left(2^j \frac{\xi_2}{\xi_1} - l\right) & \text{otherwise} \end{cases}$$

and

$$W^{(0)}{}_{j,l}(\xi) = \begin{cases} \hat{\psi}_2\left(2^j \frac{\xi_2}{\xi_1} - l + 1\right)\chi D_0(\xi) + \hat{\psi}_2\left(2^j \frac{\xi_1}{\xi_2} - l\right)\chi D_1(\xi) & \text{if } l = -2^j \\ \hat{\psi}_2\left(2^j \frac{\xi_2}{\xi_1} - l + 1\right)\chi D_0(\xi) + \hat{\psi}_2\left(2^j \frac{\xi_1}{\xi_2} - l\right)\chi D_1(\xi) & \text{if } l = 2^j - 1 \\ \hat{\psi}_2\left(2^j \frac{\xi_2}{\xi_1} - l\right) & \text{otherwise} \end{cases}$$

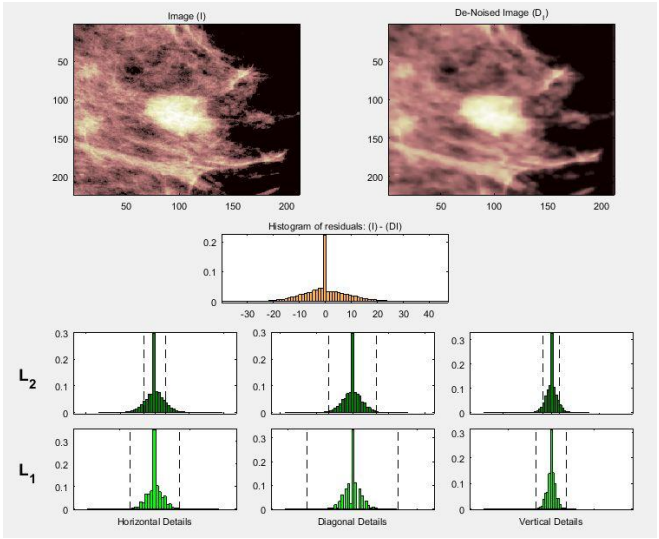

Figure 3. Shearlet based decomposed image and de-noised image

Where ψ_2, D_0, D_1 are defined in Section 2. For $1-2^j \leq l \leq 2^j-2$, each term $W^{(0)}{}_{j,l}(\xi)$ is a window function localized on a pair of trapezoids, as illustrated in Fig. 1a. When $l = -2^j$ or $l = 2^j - 1$, at the junction of the horizontal cone D_0 and the vertical cone D_1, $W^{(0)}{}_{j,l}(\xi)$ is the superposition of two such functions. Using this notation, for $j \geq 0$, $-2^j \leq l \leq 2^j-1$, $k \in Z$ 2, $d = 0, 1$, we can write the Fourier transform of the shearlets in the compact form

$$\hat{\psi}^{(d)}{}_{j,l,k}(\xi) = 2^{\frac{3j}{2}} V(2 - 2^j \xi) W^{(d)}{}_{j,l}(\xi) e^{-2\pi i \xi A_d^{-1}} B_d^{-1} k,$$

Where $V(\xi_1, \xi_2) = \hat{\psi}_1(\xi_1)\chi D_0(\xi_1, \xi_2) + \hat{\psi}_1(\xi_2)\chi D_1(\xi_1, \xi_2)$

The shearlet transform of $f \epsilon L^2(\mathbb{R}^2)$ can be computed by

$$\left(f, \hat{\psi}^{(d)}{}_{j,l,k}\right) = 2^{\frac{3j}{2}} \int_{\mathbb{R}^2} \hat{f}(\xi) \overline{V(2^{-2j}\xi) W^{(d)}{}_{j,l}} e^{-2\pi i \xi A_d^{-1}} B_d^{-1} k d\xi,$$

Indeed one can easily verify that,

$$\sum_{d=0}^{1} \sum_{l=-2^j}^{2^j-1} \left|W^{(d)}{}_{j,l}(\xi_1, \xi_2)\right|^2 = 1$$

And from this it follows that

$$|\hat{\varphi}(\xi_1, \xi_2)|^2 \sum_{d=0}^{1} \sum_{j \geq 0}^{J} \sum_{l=-2^j}^{2^j-1} |V(2^{2j}\xi_1, 2^{2j}\xi_2)| \left|W^{(d)}{}_{j,l}(\xi_1, \xi_2)\right|^2 = 1 \text{ for } (\xi_1, \xi_2) \epsilon \hat{\mathbb{R}}^2$$

Image transformation and reconstruction

Shearlets were introduced with the expressed intent to provide a highly efficient representation of images with edges. In fact, the elements of the shearlet representation form a collection of well-localized waveforms, ranging at various locations, scales and orientations, and with highly anisotropic shapes. This makes the shearlet representation particularly well adapted at representing the edges and the other anisotropic objects which are the dominant features in typical images. These properties have been theoretically quantified through the notion of sparse shearlet approximations and the shearlet analysis of singularities these properties have direct and important implications for the efficient encoding and processing of discrete data. This is demonstrated by an increasing number of very competitive numerical applications of the shearlet transform to the analysis and processing of images and other multi- dimensional data

Image transformation and reconstruction

Shearlets were introduced with the expressed intent to provide a highly efficient representation of images with edges. In fact, the elements of the shearlet representation form a collection of well-localized waveforms, ranging at various locations, scales and orientations, and with highly anisotropic shapes. This makes the shearlet representation particularly well adapted at representing the edges and the other anisotropic objects which are the dominant features in typical images. These properties have been theoretically quantified through the notion of sparse shearlet approximations and the shearlet analysis of singularities these properties have direct and important implications for the efficient encoding and processing of discrete data. This is demonstrated by an increasing number of very competitive numerical applications of the shearlet transform to the analysis and processing of images and other multi- dimensional data.

Denoising

As a first test, we evaluated the performance of our implementation of the discrete shearlet transform on a problem of image denoising, using a standard denoising algorithm based on hard threshold of the shearlet coefficients. In order to minimize latency as well as bandwidth usage on the PCIe bus, we first transferred the input image to GPU memory, then we let all the computation happen on the GPU and we finally transferred the results back to CPU memory. We have verified that both CPU and GPU implementations provide an output PSNR of 29. 9dB when the input PSNR is 22. 1dB. At these noise levels, there is no difference in PSNR between the single and the double precision implementations

Image segmentation (ROI)

Segmentation of the Region of Interest (ROI) is the crucial step in the analysis of digital mammogram images since the success of any Computer Aided Diagnostic (CADx) system depends greatly on the accuracy of the segmentation of the ROI from the mammogram images. Segmentation of mammogram images refers to segmenting the regions in the image that contains abnormalities (lesions). Analysis of these regions helps us to classify the image under consideration to be benign or malignant. Hence these regions are referred to as Region Of Interest (ROI) in the process of analyzing the mammogram images.

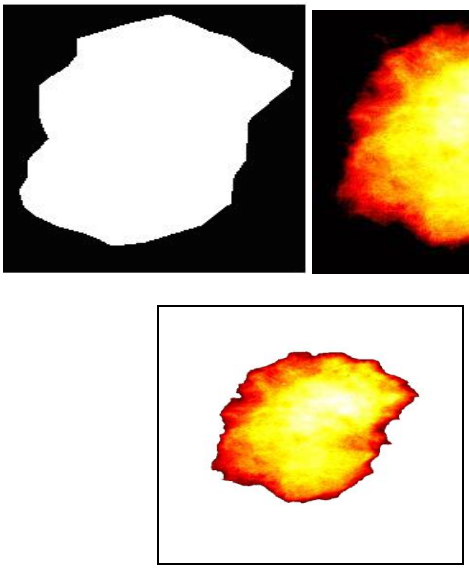

Figure4. (a)ROI selection with center axis of abnormality, (b) Region masking for the selected ROI zone, (c)ROI based extraction

Otsu's method

1. Compute histogram and probabilities of each intensity level.
2. Set up initial $\omega_i(0)$ and $\mu_i(0)$.
3. Step through all possible thresholds $t = 1 \ldots$ maximum intensity
1. Update ω_i and μ_i
2. Compute $\sigma_b^2(t)$
4. Desired threshold corresponds to the maximum $\sigma_b^2(t)$.
5. You can compute two maxima (and two corresponding thresholds). $\sigma_{b1}^2(t)$ is the greater max and $\sigma_{b2}^2(t)$ is the greater or equal maximum.
6. Desired threshold $= \dfrac{\text{threshold}_1 + \text{threshold}_2}{2}$.

Feature extraction and selection

A set of features is extracted from each mammographic region (or sample image) in the dataset because they all have been reported to be useful in separating cancerous regions from normal ones. These features include curvilinear features, texture features, Gabor features, and multi-resolution features. **Geometrical features:** orientation, area and center of mass are considered in this study. In this research, genetic algorithm is used for feature selection based on the neural network pattern classification, in which every feature is weighted by genetic algorithm. Finally, features with weights lower than a predefined threshold are eliminated. The cross-over rate and the mutation rate 0. 8 and 0. 2 are applied, respectively. The chromosome fitness is calculated according to the classification rate by a SVM classifier. Since PCA based feature selection does not attend to classification performance, in this study we prefer to use genetic algorithm for feature reduction. The above features are passed to a SEL weighted SVM and SVFNN classifier, as explained next.

Hough transform for circular shape identification

The circle Hough Transform (CHT) is a technique for detecting circles. It is a specialization of Hough Transform. The purpose of the technique is to find circles in imperfect image inputs. The circle candidates are produced by "voting" in the Hough parameter space and then select the local maxima in a so-called accumulator matrix.

In a two dimensional space, a circle can by described by:

$$(x-a)^2 + (y-b)^2 = r^2 \ldots \quad (1)$$

where (a, b) is the center of the circle, and r is the radius. If a 2D point (x, y) is fixed, then the parameters can be found according to equation(1). The parameter space would be three dimensional, (a, b, r). And all the parameters that satisfying (x, y) would lie on the surface of an inverted right-angled cone whose apex is at (x, y, 0). In the 3D space, the circle parameters can be identified by the intersection of many conic surfaces that are defined by points on the 2D circle. This process can be divided into two stages. The first stage is fixing radius then find the optimal center of circles in a 2D parameter space. The second stage is to find the optimal radius in a one dimensional parameter space.

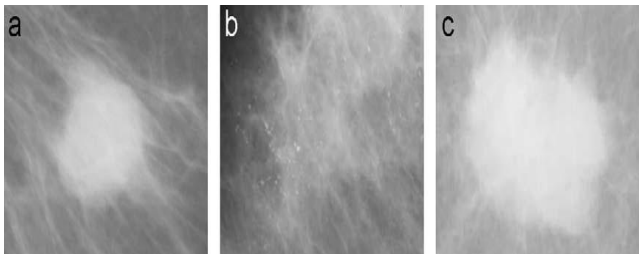

Figure 5. Typical breast abnormalities in mammograms (a) Normal, (b) micro calcified, (c) spiculated

Classification

LS- SVM classifier (least square)

LSSVMs are proposed by [17]. The most important difference between SVMs and LSSVMs is that LSSVMs use a set of linear equations for training while SVMs use a quadratic optimization problem. While formula (7) is minimized subject to formula (6) in Vapnik's standard SVMs, in LSSVMs formula (9) is minimized subject to formula (8). yi (wxi) + w0 = 1 − ξi, i = 1,..., n, (8) 1/2n i=1 αiyi (wxi) + w0 − 1 + ξi. (10) Another difference between SVMs and LSSVMs is that αi (Lagrange multipliers) are positive or negative in LSSVMs but they must be positive in SVMs. Information in detail is found in [17, 18]. 4.

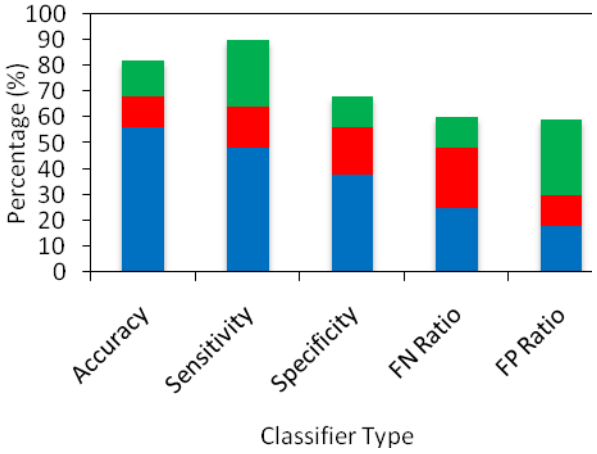

Figure 6. Classifier result

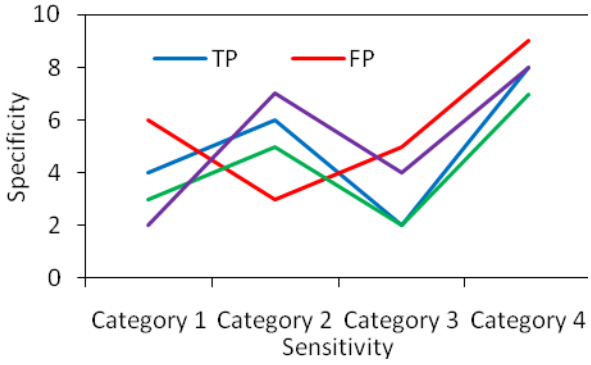

Figure 7. Specificityvs. sensitivity

Performance and metrics

The performance measures enable appropriate evaluation of the classification technique. The performance of the proposed approach for the classification of normal and abnormal images is measured by Classification Accuracy, Sensitivity and Specificity.

Table 1. SVM classification results for the image data set

Image type	Train data	Test data	Training time (sec)	Prediction Accuracy %	Prediction specificity %	Prediction sensitivity %	Error rate %
Normal	150	150	12	91. 58	94. 7	93. 2	2. 1
Micro calcified	28	28	08	93. 45	91. 6	89. 3	3. 5
Spiculated	27	28	15	92. 17	95. 4	94. 2	5. 2

Table 2. PSNR result for various image de-noising (Gaussian white noise and speckle reduction)

Sample images	Noise intensity (α)	Input PSNR (dB)	Gaussian white noise reduction(dB)	Speckle noise reduction(dB)	Computation time (sec)
Normal	1. 2	22. 1	16. 2	17. 2	14
Micro calcified	1. 8	23. 4	14. 3	16. 2	10
Spiculated mass	2. 0	21. 2	19. 2	15. 3	07

Table 3. Evaluation indices

Indices	Accuracy	Specificity	Sensitivity	FP ratio	FN ratio
Formula	$\frac{TP+TN}{TP+TN+FP+F}$	$\frac{TN}{TN+FP}$	$\frac{TP}{TP+FN}$	$\frac{TP}{TP+FI}$	$\frac{TN}{TN+FI}$

Table 4. Performance result for ROC curve evaluation

Sample Image	TP	TN	FP	FN
Normal	123	18	12	13
Micro calcified	14	07	13	02
Spiculated mass	12	02	12	04

Table. 5. Contrast thresholding values for image for the removal of background tissues

Image	Fatty	Fatty glandular	Dense glandular
Normal	35	23	10
Calcified	32	13	06
Spiculated	37	14	08

Conclusion

The work is done on a standard known database MIAS, which is readily available on the internet. In this work, SVM classifier with Shearlet transform is used. In this paper, we reviewed CAD systems for breast cancer detection and classification using ultrasound images in the literature. The techniques developed in the four stages (preprocessing, segmentation, feature extraction and selection, classification) are summarized, and their advantages and disadvantages are discussed. Different performance evaluation metrics are studied, and the future developments and trends are also investigated. The paper will be useful for the researches in BUS imaging, computer vision, image processing and radiology.

Acknowledgement

Our sincere thanks to R. RAJ JAWAHAR, Research entrepreneur, Dynamechz Research Labz. Chennai, India. for providing the technical support in conducting this work.

Appendix

A. 1. Evaluation indices

- **TP**: The number of accurately classified images, which have tumors.
- **TN**: The number of accurately classified image, which have no tumors.
- **FP**: The number of inaccurately classified images, which have tumors.
- **FN**: The number of inaccurately classified images, which have no tumors.

A. 2. Shape based features

Circularity

Circularity (C) shows how circular a certain object is. It is calculated by

$$C = \frac{4\pi A}{(pconvex)^2}$$

Where A is the object area and p_{convex} is the perimeter of its convex hull.

Circular disproportion

The circular disproportion can be obtained by

$$D = \frac{p}{2\pi R_e}$$

Where, p is the perimeter of the object under study and R is the estimated radius of a circle with the same area as the object under study. The estimated radius R_e can be obtained through where A is the area of the object under study.

Circular density

The circular density can be obtained by

$$D_e = \frac{100n}{A}$$

Where, A is the area of the object, n is the total number of points belonging to the object, and the estimated circle of radius R can be obtained through

$$R_i = \frac{R_{max}}{n} * i \text{ for } i = 1, \ldots, n$$

with center coinciding with in the center of mass of the object.

References

1. AshkanTashk, Mohammad SadeghHelfrousha, HabibollahDanyali, MojganAkbarzadeh-jahromi, Automatic detection of breast cancer mitotic cells based on the combination of textural, statistical and innovative mathematical features (2015). http://dx. doi. org/10. 1016/j. apm. 2015. 01. 051
2. Chien-Shun Lo and Chuin-Mu Wang, Support vector machine for breast MR image classification. Computers and Mathematics with Applications 64

(2012) 1153–1162. doi:10. 1016/j. camwa. 2012. 03. 033

3. Defeng Wang, Lin Shi, Pheng Ann Heng, Automatic detection of breast cancers in mammograms using structured support vector machines. Neurocomputing 72 (2009) 3296–3302. doi:10. 1016/j. neucom. 2009. 02. 015
4. BetsabehTanoori, ZohrehAzimifar, AlirezaShakibafar, SarajodinKatebi, Brain volumetry: An active contour model-based segmentation followed by SVM-based classification. Computers in Biology and Medicine 41 (2011) 619–632. doi:10. 1016/j. compbiomed. 2011. 05. 013
5. Hong-Ying Yang, Xiang-Yang Wang, Qin-Yan Wang, Xian-Jin Zhang, LS-SVM based image segmentation using color and texture information. J. Vis. Commun. Image R. 23 (2012) 1095–1112. http://dx. doi. org/10. 1016/j. jvcir. 2012. 07. 007
6. Mohsen Keshani, ZohrehAzimifar, FarshadTajeripour, Reza Boostani, Lung nodule segmentation and recognition using SVM classifier and active contour modeling: A complete intelligent system. Computers in Biology and Medicine 43 (2013) 287–30. http://dx. doi. org/10. 1016/j. compbiomed. 2012. 12. 004
7. Teresa Wu, Min HyeokBae, Min Zhang, Rong Pan, Alexandra Badea, A prior feature SVM-MRF based method for mouse brain segmentation. NeuroImage 59 (2012) 2298–2306. doi:10. 1016/j. neuroimage. 2011. 09. 053
8. Xiang-Yang Wang, Qin-Yan Wang, Hong-Ying Yang, Juan Bu, Color image segmentation using automatic pixel classification with support vector machine. Neurocomputing 74 (2011) 3898–3911. doi:10. 1016/j. neucom. 2011. 08. 004
9. Ye Chen, Judd Storrs, Lirong Tan, Lawrence J. Mazlack, Jing-Huei Lee, Long J. Lu, Detecting brain structural changes as biomarker from magnetic resonance images using a local feature based SVM approach. Journal of Neuroscience Methods 221 (2014) 22– 31. http://dx. doi. org/10. 1016/j. jneumeth. 2013. 09. 001
10. Wener Borges Sampaio, Edgar MoraesDiniz, Aristo fanes Correa Silva, Anselmo Cardoso de Paiva, Marcelo Gattass, Detection of masses in mammogram images using CNN, geostatistic functions and SVM. Computers in Biology and Medicine 41 (2011) 653–664. doi:10. 1016/j. compbiomed. 2011. 05. 017
11. Mohamed MeselhyEltoukhy, Ibrahima Faye, BrahimBelhaouari Samir, A comparison of wavelet and curvelet for breast cancer diagnosis in digital mammogram. Computers in Biology and Medicine 40 (2010) 384–391. doi:10. 1016/j. compbiomed. 2010. 02. 002
12. FatemehMoayedi, ZohrehAzimifar, Reza Boostani, SerajodinKatebi, Contourlet-based mammography mass classification using the SVM family. Computers in Biology and Medicine 40 (2010) 373–383. doi:10. 1016/j. compbiomed. 2009. 12. 006
13. Shichong Zhou, Jun Shi, Jie Zhu, Yin Cai, Ruiling Wang, Shearlet-based texture feature extraction for classification of breast tumor in ultrasound. Biomedical Signal Processing and Control 8 (2013) 688–696. http://dx. doi. org/10. 1016/j. bspc. 2013. 06. 011